Measurements of Differential Thick Target yield for C, Al, Ta, W, Pb(p,xn) reactions at 50 and 70 MeV

Naoki KAWATA, Mamoru BABA, Takao AOKI, Masayuki HAGIWARA,
Toshiro ITOGA, Naoya HIRABAYASHI, Shunsuke YONAI, Takashi NAKAMURA
Cyclotron and Radioisotope Center (CYRIC), Tohoku University
Aoba01, Aramaki, Aoba-ku, Sendai-shi, Miyagi-ken, Japan
email: nkawata@cyric.tohoku.ac.jp

2002/1/3

Differential thick target neutron yields (TTY) for C, Al, Ta, W, Pb(p,xn) reaction were measured at 50 and 70 MeV at several laboratory angles between 0- and 110-deg. with the time-of-flight method. We detrmined neutron energy spectra from ~0.6 MeV to highest secondary neutron energy.

1 Introduction

By the development of accelerator technology, the performance and the reliability of accelerators were gratly improved in recent years. High intensity and high energy accelerators are now available. Use of the accelerators are expended to material studies, medical treatment, radiobiology studies and environment science as well as nuclear physics. Now some accelerators with high energy and intensity are under construction or in e.q., Japan Proton Accelerator Research Complex (JAERI, KEK), SNS (Spallation Neutron Source, United States), and ESS (European Spallation Source).

However, nuclear data required for radiation shielding and safety design are not good enough in quality to the high energy accelerators. In particular, experimental data covering wide range of secondary neutron energies are very few. (Meigo's experimantal data for C(p, xn) at 68 MeV[10], LANL experimental data for Al, Fe, Pb(p,xn) at 113 MeV[1]) Therefor, the data for secondary neutrons spectra from the accelerator components are required.

We have started experiments on the neutron emission spectrum of the ^{nat}C(p,xn), ^{nat}Al(p,xn), ^{nat}Ta(p,xn), ^{nat}W(p,xn), and ^{nat}Pb(p,xn) reactions for tens of MeV region using the AVF cyclotron (K=110) at CYRIC[2], Tohoku University. This paper reports neutron emission spectra at 50 and 70 MeV for several laboratory angles between 0- and 110-deg.

2 Experiment

The experimental setup is shown in figure 1. A proton beam accelerated by the AVF cyclotron was transported to the target room NO.5 of CYRIC equipped with a beam-swinger system and a neutron TOF channel[3]. The beam swinger system changes the incident angle of the beam onto the target from 0-deg to 110-deg and enables to measure angular distributions with fixed detector setup.

The targets (C, Al, Ta, W, Pb) were plate of natural elements. Their sizes were shown in figure 2.

The target chamber was shielded with a 2.5 m thick concrete wall having a beam channel for collimeters. Emitted neutrons were detected by a NE213 scintillation detector, 14cm-diam $\times$ 10 cm-thick or 2 inch-diam $\times$ 2 inch-thick equipped with pulse-shape-discriminator (PSD). The larger and smaller detectors were placed around ~ 11 m and ~ 3.5 m from the target (figure **??**), respectively. The shorter flight path was adopted to measure the low energy part (~ 0.6-5 MeV) of the neutron spectrum by low pulse-height bias (~ 0.6 MeV). The TOF, PSD and pulse-height data were collected event by event as three parameter list data for off-line analysis.[4]

Table 1: Present measurement and target size

Proton energy [MeV]	Target	use	angle [deg.]	proton range [mm]	target thickness [mm]
50	C	beam dump, degrader	0, 15, 30, 45, 60, 90	11	15
	Al	beam line		11	10
	Ta	neutron source		3	3
	W	neutron source		2	3
70	C	beam dump, degrader	0, 30, 60, 90, 110	29	31
	Al	beam line		20	20
	W	neutron source		4	5
	Pb	neutron source		8	8

3 Experimental procedure

The pulse width of proton beam was generally less than 1 ns in FWHM, and the beam current on the target was around 5 ~ 10 nA. The beam current was digitized and recorded by a scaler for normalization of the neutron TOF spectrum. The TOF data for 50 MeV were obtained at six laboratory angles (0, 15, 30, 45, 60, 90), for 70 MeV at six laboratory angles (0, 30, 60, 90, 110).

4 Data analysis

Neutron TOF spectra gated by the PSD signal and the lower pulse-height bias were converted into energy spectra. The efficiency vs energy curves of the detectors were obtained by calculation with a revised version of the Monte Carlo code SCINFUL [5] that was verified to be accurate with in ± 5 % up to 80 MeV [6]. The spectra were normalized by the integrated beam current and corrected for the effect of the attenuation in the target and air using the data of LA150[6][7][8].

5 Results and discussion

In the following, experimental dadta are compared with the TTY data derived from LA150 except for ^{nat}Ta(p,xn). The TTY from LA150 was obtained by using the following equation. [9]

$$\frac{d^2Y(E_0)}{dEd\Omega} = N\int_0^T \frac{d^2\sigma\left(E_0 - \int_0^t \left(\frac{dE}{dt}\right)dt\right)}{dEd\Omega} \times e^{-N\sigma_{nonel}(E_0 - \int_0^t (\frac{dE}{dt})dt)t} dt \quad (n \bullet MeV^{-1} \bullet sr^{-1} \bullet projectile^{-1}) \quad (1)$$

where, E_0: incident particle energy [MeV], N: density of target nuclide [1/cm^3], T: thickness of the target [cm], σ_{nonel}: nonelastic cross section [cm^2], dE/dt: stopping power of incident particles [MeV/cm]

C data at 70 MeV, experimental data were compared also with Meigo's data at 68 MeV. [10]

5.1 ^{nat}C(p,xn)

Figure 2 and figure 4 show neutron spectra from ^{nat}C(p,xn) at 50 and 70 MeV respectively. Because the Q value for main component ^{12}C(p,n) is -18.1 MeV, the energy of emitted neutron is not so high. The high energy neutron component caused from ^{13}C which is included about 1.1 % naturally. Since C is light nuclide, its spectra have no evapolation peak, then neutron generation rate is low. Therefore C is suitable for beam dump, beam stopper, and the energy degrader and so on.

Figure3 and figure 5 show the comparison with LA150 and Meigo's experimental data. As you see, agreement between experimental data are very good, but the data of LA150 trace general trend but underestimate experimental data for high energy region at 50 and 70 MeV. Therefore, LA150 should be improved more to estimate neutron yield from beamdump adn so on.

5.2 ^{nat}Al(p,xn)

Figure 6 and figure 8 show neutron yields from ^{nat}Al(p,xn) at 50 and 70 MeV. Because Q value of the reaction is -5.59 MeV (is not so large), the spectra have high energy neutrons. Besides, small evapollation peaks exist abound low energy region.

Figure 7 and figure 9 show the results for the Al(p,n) reaction. For 70 MeV, a result of MCNPX calculation using LA150 as a nuclear data is also shown. The yield from equation(1) is in good agreement with the results of MCNPX underestimate experimantal data in high energy region, but similar experimental spectram in the shape and anglar distribution for all region.

5.3 ^{nat}Ta(p,xn), ^{nat}W(p,xn), ^{nat}Pb(p,xn)

Figure 10, 12, 14, and 16 show the results for ^{nat}Ta, ^{nat}W, ^{nat}Pb(p,xn), respectivelly. These neutron spectra emitted from heavy nuclides have large evapollation peak with low energy. This evapollation peak is suitable for neutron source with high intensity. Figure 11 shows anglar distribution of ^{nat}Ta. From this figure, the yields of low energy neutron is isotoropic. The angular distribution of ^{nat}W(p,xn) and ^{nat}Pb are very similar each other.

Figure 13, 15, 17 show the comparison of experimental data with the LA150 data. The data of LA150 trace generally well the experimental data although there are stil marked differences in high eneergy parts.

References

[1] C. A. GOULDING J. B. McCLELLAND G. L. MORGAN C. E. MOSS M. M. MEIER, D. A. CLARK and W. B. AMIAN. Differential neutron production cross sections and neutron yields from stopping-length targets for 113-mev protons. *Nucl. Sci. Eng.*, Vol. 102, p. 310, 1989.

[2] Cyric web page. http://www.cyric.tohoku.ac.jp.

[3] K. Kumagaik Y. Kikuchi T. Uekusa T. Uemori H. Fujisawa N. Sugimoto K. Itoh M. Baba et al. A. Terakawa, H. Suzuki. New fast-neutron time-of-flight facilities at cyric. *Nucl. Instr. and Meth.*, Vol. 491, pp. 419–425, 2002.

[4] M. Ibaraki et al. *Nucl. Sci. Eng.*, Vol. 35, p. 843, 1998.

[5] J. K. Dickens. *ORNL-6463*. Oak Ridge National Laboratory, 1988.

[6] S. Meigo. Measurements of the responce function and the detection efficiency of an ne213 scintillator for neutrons between 20 and 65 mev. *Nucl. Instr. and Meth. in Phys. Res. A*, Vol. 401, pp. 356 – 378, 1997.

[7] M. B. Chadwick, P. G. Young, R. E. MacFarlane, P. Moller, G. M. Hale, R. C. Little, A. J. Koning, S. Chiba. LA150 Documentation of Cross Sections, Heating, and Damage: Part A (Incident Neutrons). LANL Accelerator Production of Tritium Program, 1999.

[8] M. B. Chadwick, P. G. Young, R. E. MacFarlane, P. Moller, G. M. Hale, R. C. Little, A. J. Koning, S. Chiba. *LA150 Documentation of Cross Sections, Heating, and Damage: Part B (Incident Protons)*. LANL Accelerator Production of Tritium Program, 1999.

[9] Takashi Nakamura. *Radiation Physics and Accelerator safety Engineering*. Chijin Shokan, 2001.

[10] Shinichiro Meigo. In *Proc. Int. Conf. on Nuclear Data*, p. 413, Trieste, 1997.

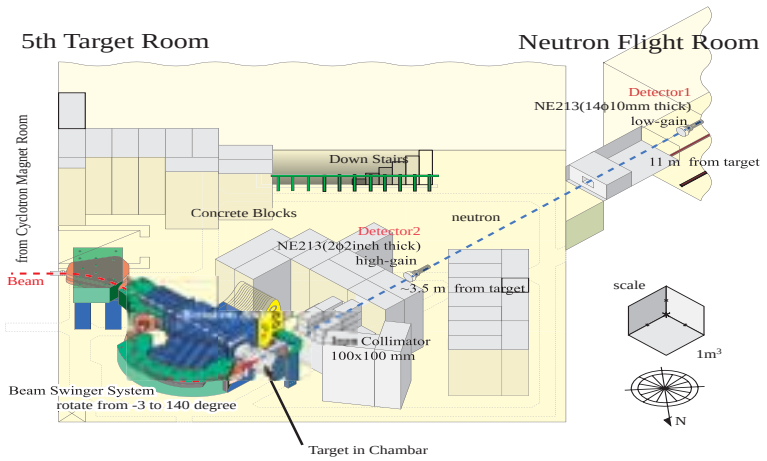

Figure 1: schimatic view of 5th target room of CYRIC

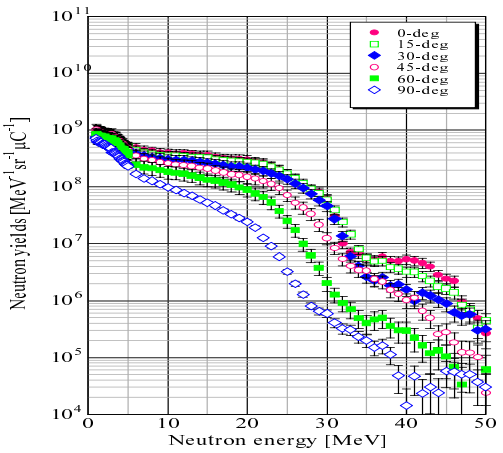

Figure 2: thick target yield for C(p,xn) at 50 MeV

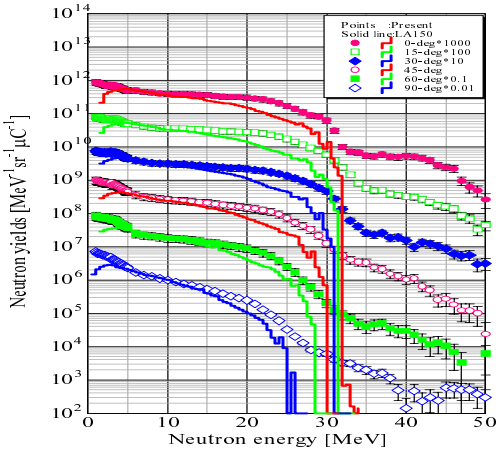

Figure 3: comparison with La150 for C(p,xn) at 50 MeV

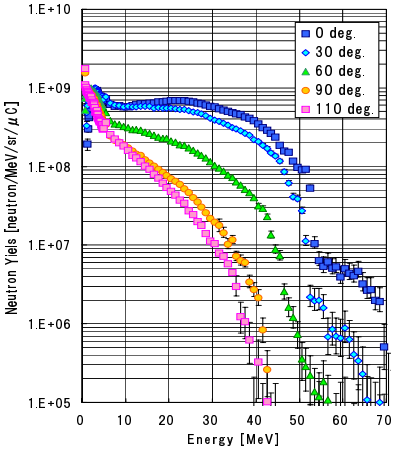

Figure 4: Thick target yield for C(p,xn) at 70 MeV

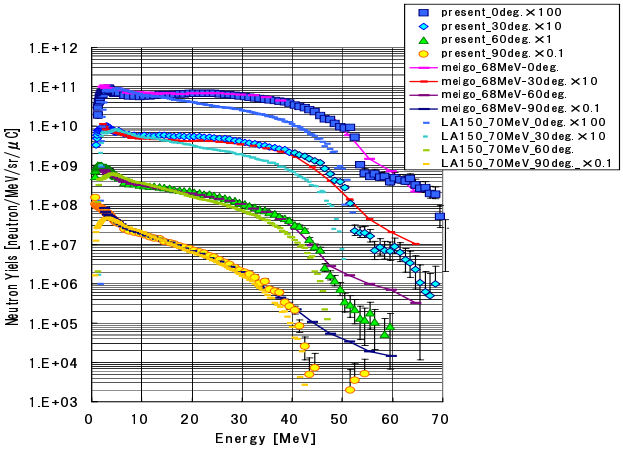

Figure 5: Comparison with La150 & Meigo's data

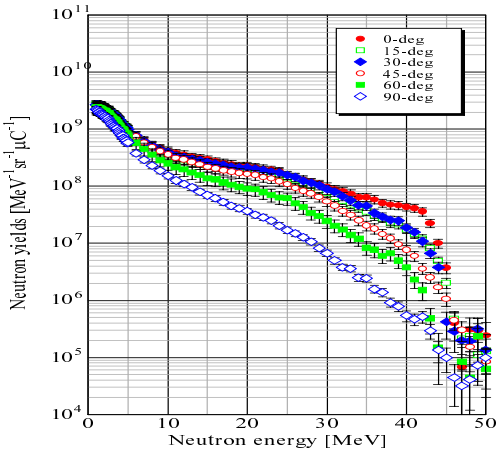

Figure 6: Thick target yield for Al(p,xn) at 50 MeV

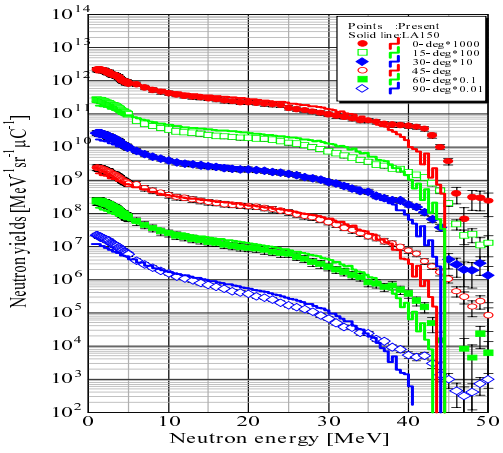

Figure 7: Comparison with La150 for Al(p,xn) at 50 MeV

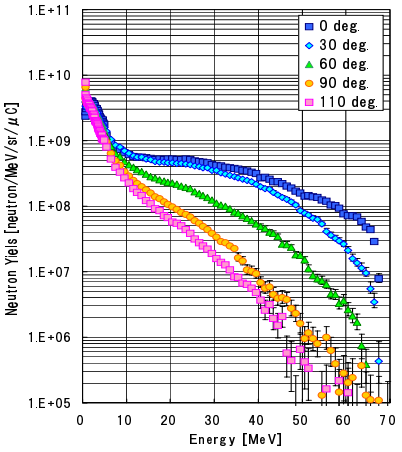

Figure 8: thick target yield for Al(p,xn) at 70 MeV

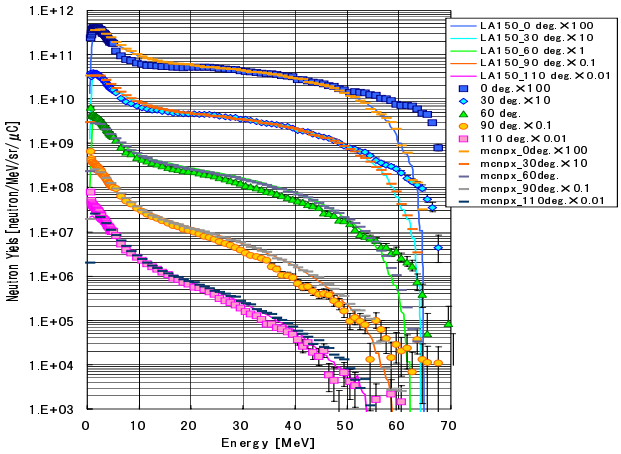

Figure 9: comparison with La150 & MCNPX for Al(p,xn) at 70 MeV

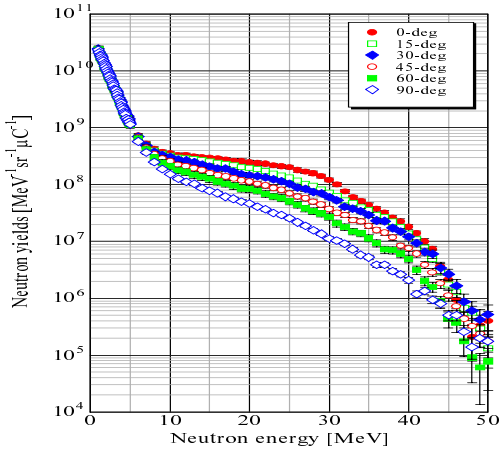

Figure 10: Thick target yield for Ta(p,xn) at 50 MeV

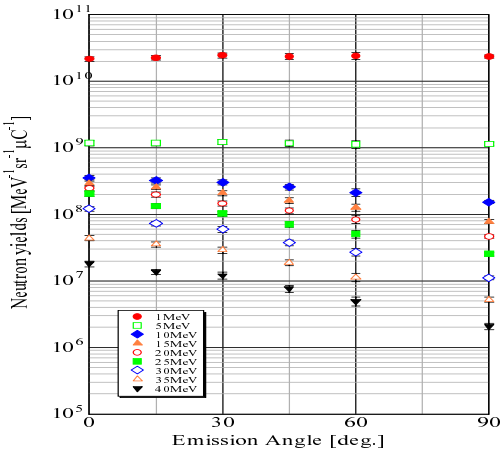

Figure 11: Angular distribution of Ta(p,xn)

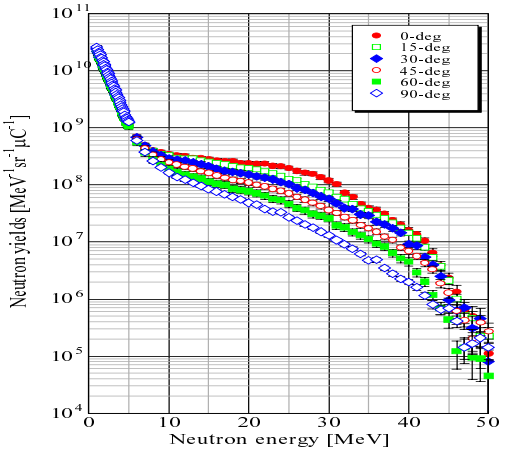

Figure 12: Thick target yield for W(p,xn) at 50 MeV

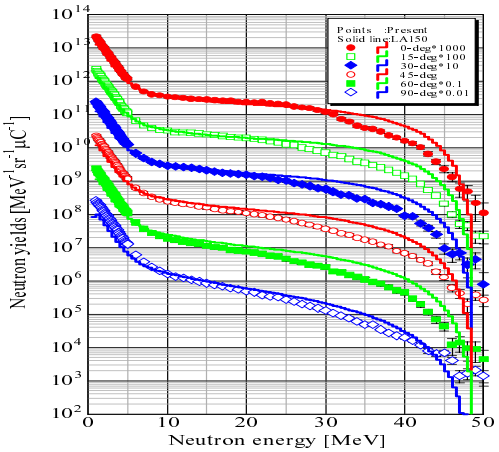

Figure 13: Comparison with La150 for W(p,xn) at 50 MeV

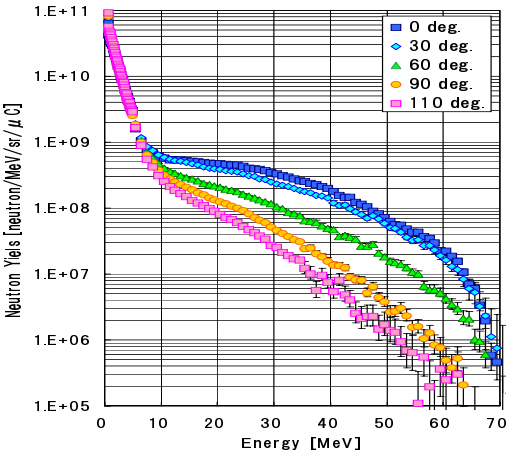

Figure 14: Thick target yield for W(p,xn) at 70 MeV

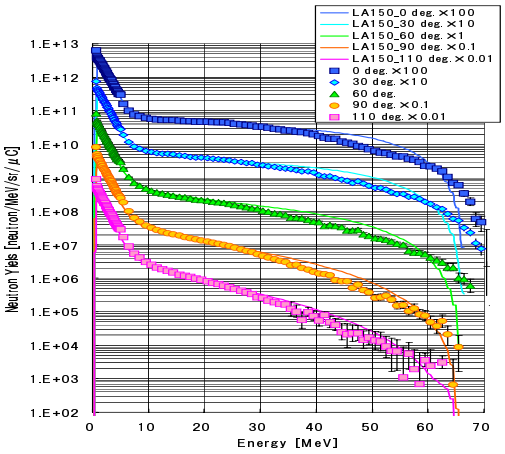

Figure 15: Comparison with La150 for W(p,xn) at 70 MeV

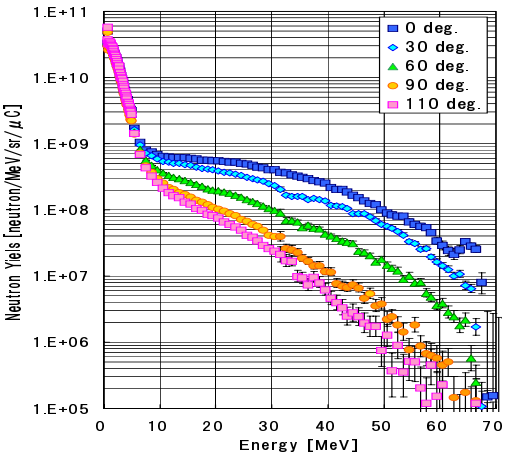

Figure 16: Thick target yield for Pb(p,xn) at 70 MeV

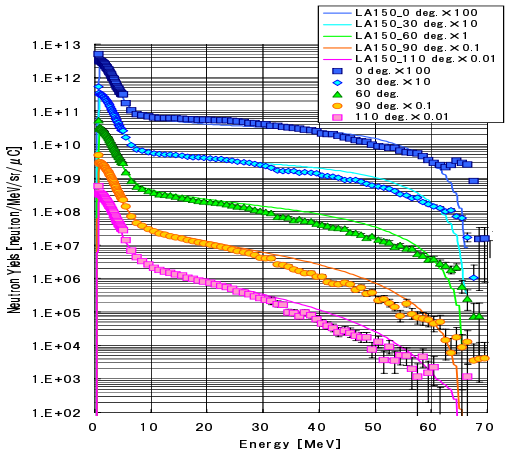

Figure 17: Comparison with La150 for Pb(p,xn) at 70 MeV